Journal of Coordination Chemistry

ISSN: 0095-8972 (Print) 1029-0389 (Online) Journal homepage: http://www.tandfonline.com/loi/gcoo20

Synthesis and spectroscopic characterization of antibacterial rhodium and ruthenium organometallics molded by C–H activation at the ortho position of a phenyl ring

Ripul Mehrotra, Satyendra N. Shukla & Pratiksha Gaur

To cite this article: Ripul Mehrotra, Satyendra N. Shukla & Pratiksha Gaur (2015) Synthesis and spectroscopic characterization of antibacterial rhodium and ruthenium organometallics molded by C–H activation at the ortho position of a phenyl ring, Journal of Coordination Chemistry, 68:4, 650-661, DOI: 10.1080/00958972.2014.999053

To link to this article: http://dx.doi.org/10.1080/00958972.2014.999053

Accepted author version posted online: 16 Dec 2014.
Published online: 09 Jan 2015.

Journal of Coordination Chemistry, 2015
Vol. 68, No. 4, 650–661, http://dx.doi.org/10.1080/00958972.2014.999053

Synthesis and spectroscopic characterization of antibacterial rhodium and ruthenium organometallics molded by C–H activation at the *ortho* position of a phenyl ring

RIPUL MEHROTRA*[,1], SATYENDRA N. SHUKLA and PRATIKSHA GAUR

Coordination Chemistry Research Lab, Department of Chemistry, Govt. Model Science College, Jabalpur, India

(*Received 1 September 2014; accepted 21 November 2014*)

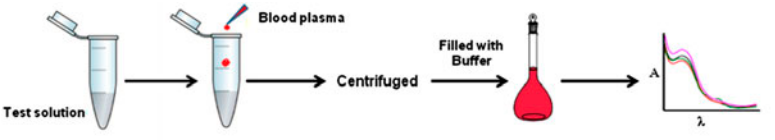

Spectrophotometric determination of organometallics in blood plasma

Cyclometalation of a pendant aromatic ring is an example of C–H bond activation. Organometallic compounds were biologically potent and may be helpful for pharmaceutical industries for biological targets.

Drug resistance in pathogens is a growing global health problem. The development of new drugs is a risky, time-consuming, and expensive process, since only a few got final approval. Organometallic compounds attracted attention due to their promising anticancer activities. In this study, four cyclometallates containing ruthenium and rhodium ions were synthesized from two phenolic azo ligands. These molecules were characterized by elemental analyses, molar conductance measurements, magnetic susceptibility, FT-IR, mass, electronic, ^{1}H, $^{13}C\{^{1}H\}$, and $^{31}P\{^{1}H\}$ NMR spectral studies. The general formula for the complexes is *trans*-$[M(PPh_3)_2(Cl)(L)]$, where M = Rh or Ru, PPh_3 = triphenylphosphine, and L = phenolic azo ligand. All the complexes possess prominent antibacterial activity against *Escherichia coli* and *Mycobacterium tuberculosis* as compared to market drugs. The interactions of rhodium derivatives with plasma–protein were also studied.

Keywords: Antibacterial; C–H activation; Organometallics; Rhodium; Ruthenium

1. Introduction

Organometallic compounds were found to be promising anticancer agents and drug candidates in therapy. The metal of organometallic compounds is kinetically stable and relatively

*Corresponding author. Email: ripul.mehrotra@gmail.com
[1]Present address: Department of Chemistry and Polymer Science, Stellenbosch University, Private Bag X1, Matieland, 7602, South Africa.

more lipophilic as compared to classical coordination complexes. Overall, organometallics offer ample opportunities in designing medicinal compounds [1–4].

C–H bond activation by metal complexes leads to many useful synthetic applications [5]. Cyclometallation of a pendant aromatic ring is one example of C–H bond activation [6]. Exhaustive reports on transition metal complexation with σ-donor ligands such as phosphine and arsine revive such studies [7, 8]. Thus, synthesis of new organometallic complexes is important. Herein, we report organorhodium and organoruthenium complexes, obtained from the reaction of 4-methyl-2-(benzylazo)phenol and 4-methyl-2-(phenylamineylazo)phenol, with precursors $[Rh(PPh_3)_3Cl]$ and $[Ru(PPh_3)_3Cl_3]$ and their antimicrobial potential.

In Pearson's classification, Rh^{3+} and Ru^{3+} both were categorized as borderline acids and prefer to bind with a soft base [9–11]. The reason behind the choice of 2-(arylazo)phenol as ligand is that simple azo-benzene binds with soft metal centers and forms stable metallacycles in coordination of monoanionic bidentate C,N–mode [12–14], as phenolate oxygen is recognized as a hard donor and stabilizes higher oxidation states of transition metals [15–17]. Therefore, we have chosen to modify phenolic azo ligands with a potential third donor site. This approach is effective in affording cyclometallates. Initially, phenolate oxygen binds to the metal center via dissociation of acidic O–H proton in N,O–fashion and generates a hydrido intermediate which is utilized to activate aryl C–H bonds, via elimination of molecular hydrogen [18].

The general notion that organometallic compounds are unstable under physiological conditions due to their sensitivity toward air and water making them unsuitable for medicinal purposes has been disproved [2]. Organometallic compounds are kinetically inert and suitable for conventional structure-based drug design, similar to traditional organic drug candidates. Thus, the aim of this study was to evaluate *in vitro* behavior of cyclometallates against bacteria to evaluate their potential in rational design of new drug candidates.

2. Experimental

2.1. *Materials*

$RhCl_3 \cdot 3H_2O$ (E. Merck), $RuCl_3 \cdot 3H_2O$ (E. Merck), triphenylphosphine (Fluka AG grade), benzylamine (Aldrich, USA), phenylhydrazine (E. Merck), sodium nitrite (Himedia), *p*-cresol (S.D. Fine, India), and Muller Hinton agar (Himedia) were used as received. Hydrochloric acid, ethanol, and routine solvents were used without purification for synthetic purposes.

2.2. *General methods*

Microanalyses (C, H, and N) were performed on an Elementar Vario EL III, Elemental analyzer. ESI-MS spectra were recorded on an Agilent 6520 Q-Tof mass spectrometer in acetonitrile and FAB spectra on a Jeol SX-102 mass spectrometer using 3-nitrobenzyl alcohol as a matrix. Electronic absorption spectra were recorded with a Shimadzu-1700 UV–vis spectrophotometer. Conductivity measurements were carried out at 25 °C on an EI-181 conductivity bridge with a dipping type cell. IR spectra were recorded from 4000 to 400 cm^{-1} using KBr pellets and a Shimadzu-8400 PC, FT-IR spectrophotometer. The far-IR spectra

of the complexes were recorded using polyethylene pellets from 500 to 100 cm^{-1} on a Nicolet Mega-550 FT-IR Instrument. ^{1}H and $^{13}C\{^{1}H\}$ NMR spectra were recorded in $CDCl_3$ on a Bruker DRX-300 NMR spectrometer. The chemical shifts were expressed as δ (ppm) from internal reference standard TMS. The $^{31}P\{^{1}H\}$ NMR spectra for **1** and **3** were recorded in DMSO-d_6 on a Jeol GSX-400 instrument at room temperature using *ortho*-phosphoric acid as reference. Gouy's method was employed for the measurement of magnetic susceptibility using $Hg[Co(NCS)_4]$ as standard. Diamagnetic corrections were made by using Pascal's constant.

2.3. *Statistical analysis*

Statistical analysis was performed by one-way analysis of variance (ANOVA) using GraphPad Prism 6 (version 6.04 (Trial) for Windows; GraphPad Software, Inc., CA). Differences were considered statistically significant at P values of <0.05.

2.4. *Preparation of phenolic azo ligands*

The ligands 4-methyl-2-(benzylazo)phenol (H_2L^1) and 4-methyl-2-(phenylamineylazo)phenol (H_2L^2) were prepared by coupling of *p*-cresol with diazotized benzylamine and phenylhydrazine, respectively, according to standard procedure. The solids obtained were collected by filtration, washed with ice cold water : ethanol (1 : 1) mixture, and dried in vacuum.

H_2L^1: Yield: 0.0986 g (87.1%). IR: (KBr, cm^{-1}) 3380(s), ν(Ar–OH); 2872(s), 2845(s), $\nu(CH_2)$; 1428(w), ν(N=N); 1322(s), ν(Ar–C–O). ^{1}H NMR (300 MHz, δ, $CDCl_3$): 10.82(brs, 1H, Ar-OH); 6.48–6.02(m, 8H, Ar–H); 4.84(s, 2H, CH_2); 1.72(s, 3H, CH_3). $^{13}C\{^{1}H\}$ NMR (300 MHz, δ, $CDCl_3$): 168.8, 152.2, 147.6, 142.3, 140.1, 138.9, 137.3, 137.0, 129.4, 126.3 (Ar–C); 54.3(C-CH_2); 21.3(C–CH_3). Electronic spectra (λ_{max}, nm (ε in M^{-1} cm^{-1})) in acetonitrile: 308(854), 273(963). Anal. Calcd for $C_{14}H_{14}N_2O$ ($M\tau$ = 226): C, 74.31; H, 6.24; N, 12.38. Found: C, 74.22; H, 6.21; N, 12.28. ESI-MS (*m/z*): $[C_{14}H_{14}N_2O + H]^+ = 227$.

H_2L^2: Yield: 0.0944 g (83.2%). IR: (KBr, cm^{-1}) 3452(w), ν(–NH); 3386(s), ν(Ar–OH); 1426(w), ν(N=N); 1325(s), ν(Ar–C–O). ^{1}H NMR (300 MHz, δ, $CDCl_3$): 10.86(brs, 1H, Ar–OH); 6.81–6.23(m, 8H, Ar–H); 5.56(brs, 1H, NH); 1.76(s, 3H, CH_3). $^{13}C\{^{1}H\}$ NMR (300 MHz, δ, $CDCl_3$): 166.7, 150.1, 146.3, 141.9, 138.3, 133.9, 133.0, 130.3, 127.4, 124.8 (Ar–C); 21.4(C-CH_3). Electronic spectra (λ_{max}, nm (ε in M^{-1} cm^{-1})) in acetonitrile: 310 (878), 274(972). Anal. Calcd for $C_{13}H_{13}N_3O$ ($M\tau$ = 227): C, 68.71; H, 5.77; N, 18.49. Found: C, 68.62; H, 5.73; N, 18.42. ESI-MS (*m/z*): $[C_{13}H_{13}N_3O + H]^+ = 228$.

2.5. *Preparation of the complexes*

Complexes **1–4** with general formula *trans*-$[M(PPh_3)_2(Cl)(L)]$ were prepared with selected rhodium and ruthenium precursor, where M = Rh/Ru and L = phenolic azo ligand. Appropriate quantities of phenolic azo ligand (0.5 mM) (H_2L^1 for **1** and **2** and H_2L^2 for **3** and **4**) dissolved in toluene (~35 mL) were mixed with triethylamine (1.1 mM) and the corresponding precursor (0.5 mM) $[RhCl(PPh_3)_3]$ [19] (for **1** and **3**) and $[RuCl_3(PPh_3)_3]$ [20] (for **2** and **4**). The reaction mixture was kept under reflux for 7–8 h. The volume of the resulting solution was reduced under vacuum. The solid obtained was filtered, washed with toluene : acetonitrile (1 : 1) solvent mixture, and dried in vacuum.

2.5.1. 1: *trans*-bis(triphenylphosphine)chloro(4-methyl-2-(benzylazo)phenol rhodium (III). Color: orange red, Yield: 0.3888 g (87.6%); m.p. > 220 °C. IR: (KBr, cm^{-1}) 2874(s), 2846(s), $\nu(CH_2)$; 1416(w), ν(N=N); 1346(s), ν(Ar–C–O); 742(s), 692(s), 515(s), ν(*trans*-Rh$(PPh_3)_2$); 456(s), ν(Rh–O); 336(s), ν(Rh–Cl); 276(s), ν(Rh–N). ^{1}H NMR (300 MHz, δ, $CDCl_3$): 8.88–6.30(m, 37H, Ar–H); 4.90(dd, 2H, CH_2); 1.74(s, 3H, CH_3). $^{13}C\{^1H\}$ NMR (300 MHz, δ, $CDCl_3$): 174.9–130.1 (Ar–C); 54.7(C–CH_2); 21.6(C–CH_3). $^{31}P\{^1H\}$ NMR (400 MHz, δ, DMSO-d_6): 30.08. Electronic spectra (λ_{max}, nm (ε in M^{-1} cm^{-1})) in acetonitrile: 684(62), 546(255), 409(617), 336(963), 296(1124). Λ_M at 25 °C (in μS/cm): 24 in DMSO, 62 in acetonitrile. Anal. Calcd for $C_{50}H_{42}N_2OClP_2Rh$ (Mτ = 887): C, 67.69; H, 4.77; N, 3.16. Found: C, 67.60; H, 4.74; N, 3.22. FAB-MS (*m/z*): $[C_{50}H_{42}N_2OCl^{37}P_2Rh]^+$ = 889, $[C_{50}H_{42}N_2OClP_2Rh + H]^+$ = 888.

2.5.2. 2: *trans*-bis(triphenylphosphine)chloro(4-methyl-2-(benzylazo)phenol ruthenium (III). Color: blood red, Yield: 0.3240 g (73.2%); m.p. > 220 °C. IR: (KBr, cm^{-1}) 2870(s), 2846(s), $\nu(CH_2)$; 1412(w), ν(N=N); 1340(s), ν(Ar–C–O); 740(s), 690(s), 518(s), ν(*trans*-Ru$(PPh_3)_2$); 556(s), ν(Ru–O); 332(s), ν(Ru–Cl); 277(s), ν(Ru–N). Electronic spectra (λ_{max}, nm (ε in M^{-1} cm^{-1})) in acetonitrile: 486(106), 401(506), 346(681), 299(954). Λ_M at 25 °C (in μS/cm): 18 in DMSO, 53 in acetonitrile. μ_{eff} = 1.82 BM. Anal. Calcd for $C_{50}H_{42}N_2OClP_2Ru$ (Mτ = 885): C, 67.83; H, 4.78; N, 3.16. Found: C, 67.88; H, 4.76; N, 3.20. FAB-MS (*m/z*): $[C_{50}H_{42}N_2OClP_2Ru^{104}]^+$ = 888, $[C_{50}H_{42}N_2OCl^{37}P_2Ru]^+$ = 887, $[C_{50}H_{42}N_2OClP_2Ru + H]^+$ = 886, $[C_{50}H_{42}N_2OClP_2Ru^{96}]^+$ = 880.

2.5.3. 3: *trans*-bis(triphenylphosphine)chloro(4-methyl-2-(phenylamineylazo)phenol rhodium(III). Color: orange, Yield: 0.3844 g (86.6%); m.p. > 220 °C. IR: (KBr, cm^{-1}) 3450(w), ν(–NH); 1414(w), ν(N=N); 1351(s), ν(Ar–C–O); 744(s), 695(s), 520(s), ν(*trans*-Rh$(PPh_3)_2$); 450(s), ν(Rh-O); 334(s), ν(Rh–Cl); 278(s), ν(Rh–N). ^{1}H NMR (300 MHz, δ, $CDCl_3$): 9.12–7.27(m, 37H, Ar–H); 6.01(t, 1H, –NH); 1.74(s, 3H, CH_3). $^{13}C\{^1H\}$ NMR (300 MHz, δ, $CDCl_3$): 174.6–128.4(Ar–C); 21.8(C–CH_3). $^{31}P\{^1H\}$ NMR (400 MHz, δ, DMSO-d_6): 30.12. Electronic spectra (λ_{max}, nm (ε in M^{-1} cm^{-1})) in acetonitrile: 679(54), 544(251), 403(611), 338(1004), 300(1086). Λ_M at 25 °C (in μS/cm): 22 in DMSO, 58 in acetonitrile. Anal. Calcd for $C_{49}H_{41}N_3OClP_2Rh$ (Mτ = 888): C, 66.26; H, 4.65; N, 4.73. Found: C, 66.30; H, 4.66; N, 4.76. FAB-MS (*m/z*): $[C_{49}H_{41}N_3OCl^{37}P_2Rh]^+$ = 890, $[C_{49}H_{41}N_3OClP_2Rh^{103}]^+$ = 889.

2.5.4. 4: *trans*-bis(triphenylphosphine)chloro(4-methyl-2-(phenylamineylazo)phenol ruthenium(III). Color: red, Yield: 0.3332 g (75.2%); m.p. > 220 °C. IR: (KBr, cm^{-1}) 3455 (w), ν(–NH); 1408(w), ν(N=N); 1348(s), ν(Ar–C–O); 741(s), 692(s), 516(s), ν(*trans*-Ru$(PPh_3)_2$); 554(s), ν(Ru–O); 338(s), ν(Ru–Cl); 280(s), ν(Ru–N). Electronic spectra (λ_{max}, nm (ε in M^{-1} cm^{-1})) in acetonitrile: 474(111), 399(508), 342(672), 301(899). Λ_M at 25 °C (in μS/cm): 16 in DMSO, 51 in acetonitrile. μ_{eff} = 1.79 BM. Anal. Calcd for $C_{49}H_{41}N_3OClP_2Ru$ (Mτ = 886): C, 66.40; H, 4.66; N, 4.74. Found: C, 66.33; H, 4.66; N, 4.72. FAB-MS (*m/z*): $[C_{49}H_{41}N_3OClP_2Ru^{104}]^+$ = 889, $[C_{49}H_{41}N_3OCl^{37}P_2Ru]^+$ = 888, $[C_{49}H_{41}N_3OClP_2Ru + H]^+$ = 887, $[C_{49}H_{41}N_3OClP_2Ru^{96}]^+$ = 881.

3. Results and discussion

3.1. *Synthesis and physicochemical characterization*

The phenolic azo ligands H_2L^1 and H_2L^2, where H_2 stands for two hydrogens (one phenolic and one phenyl (at 2' position)), were synthesized by coupling of *p*-cresol with the corresponding diazotized amines at 0 °C. These ligands were utilized in the preparation of **1–4** with $[RhCl(PPh_3)_3]$ and $[RuCl_3(PPh_3)_3]$ precursors. The reaction proceeds smoothly in the presence of triethylamine to afford organometallic complexes, *trans*-$[M(PPh_3)_2(Cl)(L)]$ (where M = Rh or Ru). The desired product was recovered as a solid under vacuum evaporation and purified through diffusing Et_2O in DCM solution at room temperature. The crystal attempts failed, and the solid obtained was only a powder. All the complexes are stable in air as solids and soluble in common organic solvents such as $CHCl_3$, AcCN, EtOH, DCM, and DMSO.

Empirical formulas of H_2L^1, H_2L^2, and **1–4** were in agreement with elemental analyses. Molecular weights were determined by mass spectroscopy. In mass spectra of **1-4**, isotopic patterns for Ru- and Rh-containing ions were clearly identified because there are few relevant ions. Ruthenium has six isotopes with significant natural abundance (>15% from 96 to 104 amu), rhodium has one (103 amu), and Cl has two (35 and 37 amu) [21]. The molar conductivities for **1–4** were between 16 and 24 μS/cm in DMSO and 51 and 62 μS/cm in acetonitrile, being in the range suggested for non-electrolytes [22].

3.2. *Spectral studies*

3.2.1. Infrared spectral analysis. In FT-IR spectra of H_2L^1 and H_2L^2, the strong band at 1322 cm^{-1}, attributed to phenolic C–O stretch [23], shifted to higher wave numbers by 18–26 cm^{-1} in spectra of the complexes, indicating that one of the binding sites was phenolic oxygen. The stretching band for phenolic −OH at ~3380 cm^{-1} in free ligand vanished in **1–4** [24]. This was further in support with involvement of phenolate oxygen in coordination and confirmed with the band for ν(M–O). This band was observed at 450 and 550 cm^{-1} in rhodium and ruthenium complexes, respectively [25, 26]. Another band observed for H_2L^1 and H_2L^2 at ~1428 cm^{-1} corresponding to N=N unsymmetrical stretch [27] is weak, probably due to non-polar nature, and shows negative shifts by 12–18 cm^{-1} in **1–4**. This was an indication for involvement of N=N as another binding site and in support with ν(M–N) stretch at ~280 cm^{-1} [25].

Two sharp vibrations at 2872 and 2845 cm^{-1} in H_2L^1 assigned for $\nu(CH_2)$ and the weak band in H_2L^2 at 3452 cm^{-1} attributed to –NH were at almost the same positions, in the corresponding complexes. A sharp vibration at 340 cm^{-1} in **1–4** was assigned to ν(M–Cl). Each complex displayed strong absorptions near 520, 690, and 740 cm^{-1}, attributed to vibrations arising from *trans*-$M(PPh_3)_2$ moiety [28, 29].

3.2.2. Electronic spectral analysis and magnetic moment. In electronic spectra of H_2L^1 and H_2L^2, two bands in the UV region at 274 and 308 nm were attributed to $\pi \rightarrow \pi^*$ and $n \rightarrow \pi^*$ transitions, respectively. Shifting of these bands in **1–4** with color change authenticates coordination.

Complexes **1** and **3** were diamagnetic (low-spin d^6, $S = 0$), as expected for low-spin Rh (III) compounds. In the visible region, broad bands with low extinction coefficients were

observed between 684 and 679 nm, 546 and 544 nm, and 409 and 403 nm, assigned to $^1A_{1g} \rightarrow {}^3T_{1g}$, $^1A_{1g} \rightarrow {}^1T_{1g,}$ and $^1A_{1g} \rightarrow {}^1T_{2g}$ transitions, respectively, of Rh(III) [30]. However, higher energy absorption bands below 340 nm were attributed to $\pi \rightarrow \pi^*$ intraligand transitions in coordinated π-acidic imine ligand [31–33].

Complexes **2** and **4** were paramagnetic with magnetic moments 1.82 and 1.79 BM, respectively, for low-spin (d^5) Ru(III) complexes. Four bands appeared between 486 and 474 nm, 401 and 399 nm, 346 and 342 nm, and 301 and 299 nm. The lowest energy absorption bands, assigned to $^2T_{2g} \rightarrow {}^4T_{1g}$ and $^2T_{2g} \rightarrow {}^4T_{2g}$ transitions of Ru(III), were observed as shoulders on the charge-transfer band [34]. The electronic spectral assignment suggested octahedral environment around the metal.

3.2.3. NMR spectral studies. In the ^{1}H NMR spectrum of the ligands, the down-field signal at $\delta = 10.82$ ppm due to phenolic proton [8] disappeared in **1** and **3** indicating deprotonation of Ar–OH and involvement of phenolate oxygen in complexation. The methylene protons observed as a singlet at $\delta = 4.84$ ppm in free H_2L^1 appeared as a doublet of doublets in **1** at $\delta = 4.90$ ppm. The broad signal at $\delta = 5.56$ ppm for −NH in free H_2L^2 was observed as a triplet in **3**, due to nitrogen nuclear spin ($I = 1$) [24]. The aromatic region ($\delta = 6.0$−9.0 ppm) is complicated due to overlapping of several signals (since electronic environments of many aromatic hydrogens are similar) which makes difficult identifying individual resonances. Signals for methyl protons were observed at $\delta = 1.72$ ppm [28].

In $^{13}C\{^1H\}$ NMR spectra of **1** and **3**, methyl carbon in *p*-cresol fragment showed an isolated signal near $\delta = 21$ ppm. The resonances observed between $\delta = 125$ and 175 ppm were assigned to Ar–C, out of which the most deshielded one (near $\delta = 175$ ppm) was assigned to the metallated carbon [28]. In H_2L^1 and **1**, the $-CH_2$ carbon appeared at $\delta = 54$ ppm [8].

In $^{31}P\{^1H\}$ NMR spectra of **1** and **3**, a phosphine doublet was observed at $\delta = 30.08$ and 30.12 ppm, with a ^{31}P–^{103}Rh coupling constant of 115 and 103 Hz, respectively [35]. The presence of magnetically equivalent phosphorus atoms suggested that triphenylphosphine groups are in a *trans* position to each other. The NMR results are, therefore, in excellent agreement with the composition and stereochemistry of **1** and **3**.

3.3. *Structure of ligands, diamagnetic Rh(III), and paramagnetic Ru(III) complexes*

On the basis of elemental analyses, conductivity experiments and spectroscopic studies (FT-IR, UV–vis, mass, and NMR) the most plausible structure for H_2L^1, H_2L^2, and Rh(III) complexes **1** and **3** are suggested in figure 1.

Signals in NMR spectra of Ru(III) complexes (**2** and **4**) were too broad and shifted from their original positions, due to paramagnetism [26, 36]. On the basis of UV–vis and FT-IR studies, it was evident that probably, two Cl^- were replaced along with two H^+ ions (one of Ar–OH and second due to C–H bond activation) during complexation. This view was verified qualitatively by $AgNO_3$ test [21, 25]. Thus, binding modes of **2** and **4** were concluded on the basis of elemental analyses, conductivity experiments, and spectroscopic (FT-IR, UV–vis, and FAB-Mass) studies as suggested in figure 1.

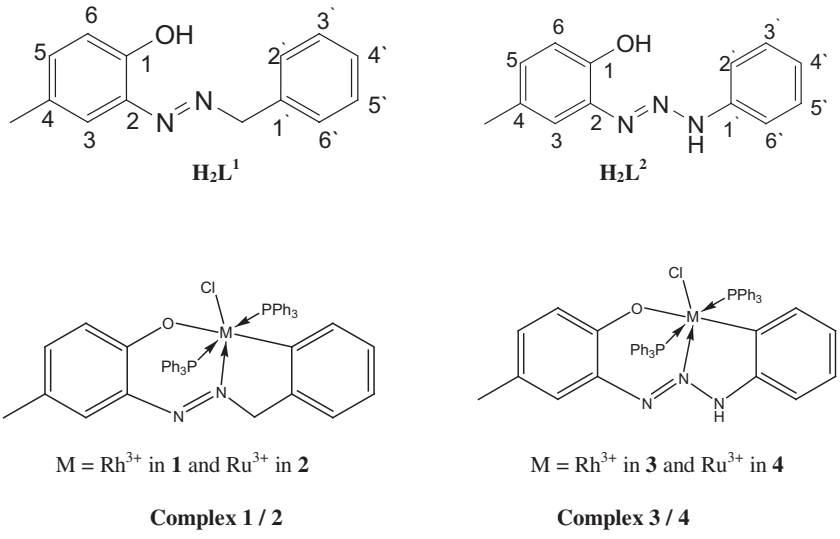

Figure 1. Proposed structure of H_2L^1, H_2L^2, and **1–4**.

3.4. In vitro *antibacterial assay and MIC evaluation*

Complexes **1–4**, precursors ([$RhCl(PPh_3)_3$] and [$RuCl_3(PPh_3)_3$]), and ligands (H_2L^1 and H_2L^2) were screened for antibacterial properties against *E. coli*, MTCC 1304, and *M. tuberculosis*, ATCC 27294 at concentration of 2.5 and 50 μg/mL in DMSO by agar well diffusion method. The Muller Hinton (MH) and Lowenstein–Jensen medium [37] were used for the growth of *E. coli* and *M. tuberculosis*. A 50-μL bacterial culture containing approximately 10^5 CFU (colony forming unit) was applied to the plate by spreading with a cotton swab [38]. The wells created (diameter of 6.0 mm) in agar slab were filled with 50 μL of test and control. A 2.0 μg/mL solution of ciprofloxacin (CP), gatifloxacin (GT), isoniazid, and rifampicin was used as positive control with respect to sensitivity of bacterial strains. DMSO served as a negative control. All plates were kept at 4 °C for 20 min and then incubated at 37 °C for the same time. Results were obtained as inhibition zone, measured in mm.

The minimum inhibitory concentration (MIC) test was used to establish the bioactivity and effectiveness of **1–4** against studied pathogen. The successive dilution method was used for MIC evaluation [39] and reported as concentration of higher dilution tube in which bacterial growth was absent. Complex **1** was the most active to inhibit *E. coli* at MIC = 0.31 μg/mL and *M. tuberculosis* at 3.12 μg/mL (table 1).

Table 1. MIC evaluation of **1–4** and standard drugs.

	MIC of compounds (μg/mL)							
Bacterial strains	**1**	**2**	**3**	**4**	CP	GT	Isoniazid	Rifampicin
E. coli	0.31	0.62	0.62	1.25	0.25	0.25	ND	ND
M. tuberculosis	3.12	6.25	6.25	25.0	ND	ND	0.10	0.20

ND = not determined.

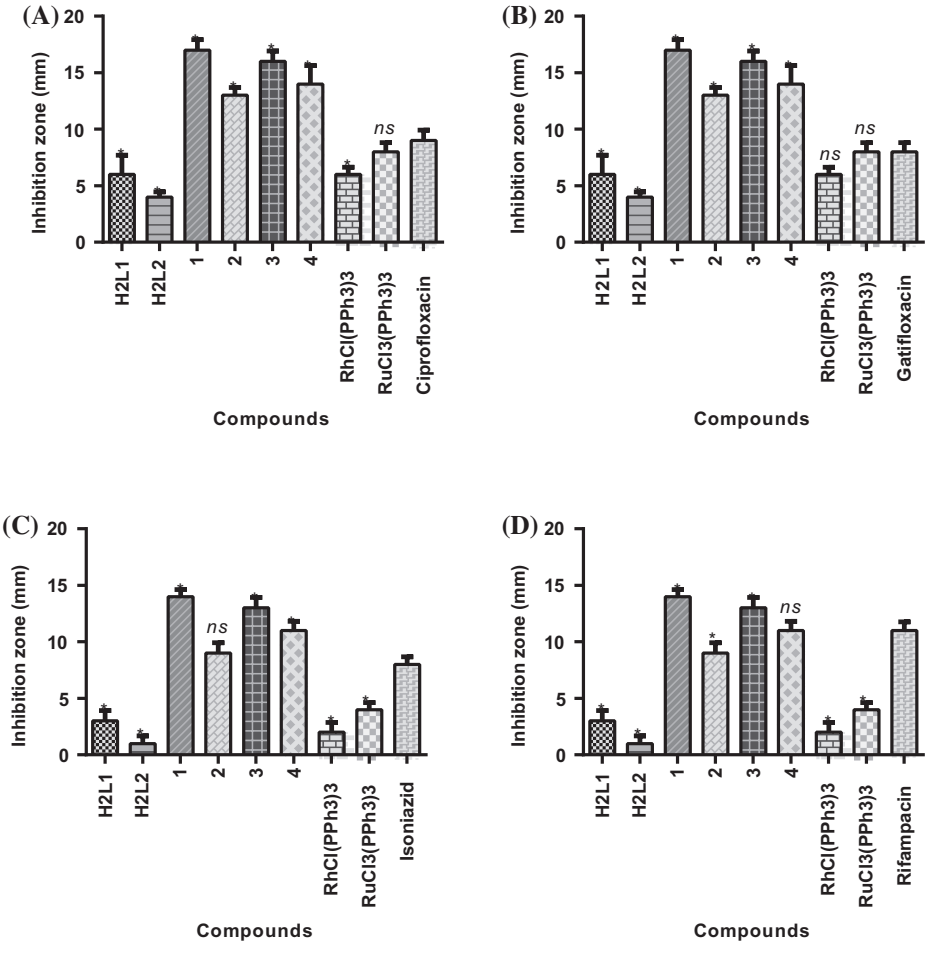

Figure 2. Effect on inhibition zone at concentration 2.5 μg/mL against *E. coli* and 50 μg/mL against *M. tuberculosis* in comparison to (A) CP, (B) GT, (C) isoniazid, and (D) rifampicin. The values of zone of inhibition were obtained by subtracting control (DMSO). Statistics points are the average values of three independent experiments (mean ± standard deviation; $n = 3$). *, $p < 0.05$; *ns* = not significant.

Figure 2 summarizes the inhibitory spectrum of compounds against tested strains. The enhanced antimicrobial activity of **1–4** as compared to corresponding precursors was perhaps due to increased liphophilicity causing permeability barrier breakdown and enzyme binding inhibition leading to cell death [40]. The inhibitory action of cyclometallates is not only because of stable bystander ligand, but also due to the hydrophobicity of the metal–carbon bond with a phenyl ring.

The significant increase ($p < 0.0001$) in zone inhibition obtained for **1** against *E. coli* was 17 mm as compared to CP and GT [figure 2(A) and (B)]. Similarly, for **2,** it was 13 mm ($p < 0.01$), **3** (16 mm; $p < 0.0001$) and **4** (14 mm; $p < 0.001$). For *M. tuberculosis,* the values of inhibition zone (14 mm) obtained with **1** were most significant ($p < 0.0001$ and $p < 0.01$), in comparison to isoniazid and rifampicin, respectively.

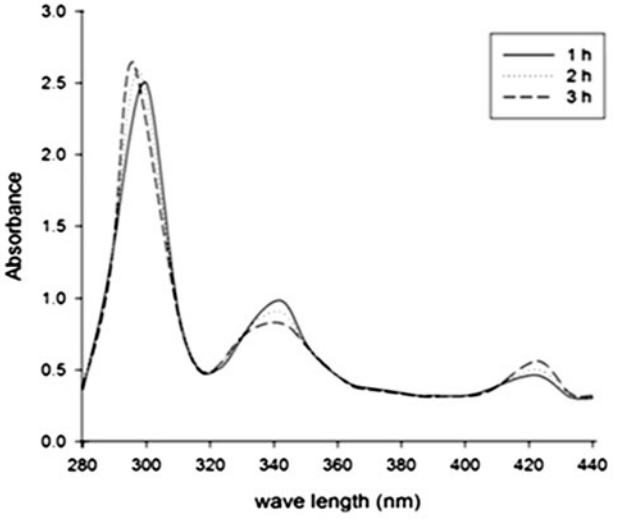

Figure 3. Time dependent UV–vis absorption spectra of **1** in phosphate buffer.

3.5. *Stability studies for rhodium compounds in buffer solutions*

The biosusceptibility of organorhodium derivatives against bacteria was substantial as compared to $[RhCl(PPh_3)_3]$ (figure 2). These results encouraged us to examine the plasma–protein interaction for **1** and **3** in comparison with $[RhCl(PPh_3)_3]$. The stability of rhodium derivatives in buffer solution was monitored through UV–vis absorption method [41]. 0.10 g of complexes was first dissolved in a minimum amount of DMSO and then diluted with 0.1 M sodium phosphate buffer (3.1 g $NaH_2PO_4{\cdot}H_2O$ and 10.9 g Na_2HPO_4 (anhydrous) in distilled water to a volume of 1 L, pH 7.4) up to 5 mL. The samples were analyzed by monitoring electronic spectra of resulting mixtures over 24 h at 37 °C.

In freshly prepared buffer solution, **1** showed two absorptions in the visible region, one at 300 nm and another at 342 nm. In the first 3 h, after dissolution of **1**, the band observed at high energy shows a clear blue shift with an increase in absorption maximum, while at the same time, the band at 342 nm starts decreasing and another new band was formed at 423 nm. The clear isosbestic points (at 330 and 412 nm) indicate equilibrium between starting compound and hydrolysis product [42] (figure 3). No discrete spectral changes were noticed in the next two days. The hydrolysis profile of **3** was similar to **1**. The presence of strong phosphine ligands confers favorable pharmacological properties [43, 44], whereas –Cl may act as a weaker ligand and dissociate easily. Probably, this facilitates Rh(III) ion to bind biomolecules.

For solution of $[RhCl(PPh_3)_3]$ in phosphate buffer, the first hydrolysis step was completed within 5 min and much faster than that observed under physiological conditions. After 2 h, the second hydrolysis occurs, during which the red solution becomes dark. No further spectral changes were noticed over the next two days. The fast change in $[RhCl(PPh_3)_3]$ might be from the unstable oxidation state of Rh(I), since it easily undergoes oxidation to give the corresponding octahedral Rh(III) species that undergoes substitution at a lower rate [45]. In another experiment, Tris–HCl buffer (5 mM Tris–HCl, 50 mM NaCl, pH 7.1) was used instead of phosphate buffer to rule out the possibility of phosphate interaction

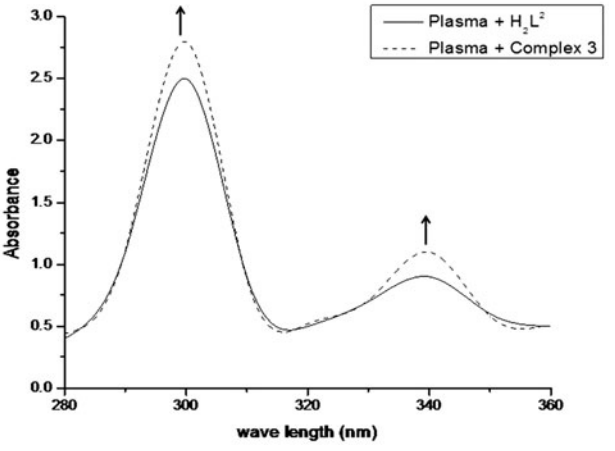

Figure 4. UV absorption spectra of plasma interaction with H_2L^2 and **3**.

with Rh(III). The similar absorption profiles with both buffers indicated the interaction of Rh(III) with protein.

3.6. *Spectrophotometric determination of rhodium complexes in blood plasma*

A 0.1% solution of **1** and **3** was prepared in DMSO and optimized by standard procedure [46]. Blood plasma [obtained from a local pathological laboratory] (1.0 mL) was mixed with different volumes of 0.1% **1** and **3** and incubated at 37 °C for 1 h. The samples were then centrifuged at 1500 rpm for 30 min. Supernatant was separated, filtered, and then transferred into a 5-mL volumetric flask. The flask was filled with 0.1 M sodium phosphate buffer. Electronic spectra of samples were recorded in the UV range and compared against plasma blank in the presence of ligand (scheme 1).

The UV spectrum of samples consists of two major bands (figure 4), one higher energy band at 300 nm due to the $\pi \rightarrow \pi^*$ transition in the aromatic ring and the other at 340 nm due to $n \rightarrow \pi^*$ transition. The intensities of these bands increase with concentration of complex and pH (up to 8), which shows a clear hyperchromic shift, confirming that plasma proteins interfere with complexes [39].

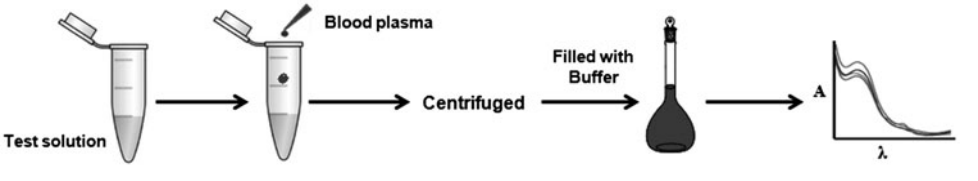

Scheme 1. Spectrophotometric determination of the organometallic complexes in blood plasma.

4. Conclusion

Four rhodium- and ruthenium-containing cyclometallates have been synthesized through C–H bond activation and characterized by spectroscopic methods. The $M(PPh_3)_2$ moiety attains *trans*-configuration in all compounds. The coordination sites to metal ion are phenolic oxygen and phenyl carbon. These complexes are novel due to their specific structure and biological activity against bacteria. Compounds **1–4** showed higher potency compared to antibiotics and precursors. Their action is not only due to improved lipophilicity but also because of the hydrophobicity of the metal-carbon bond, which is perhaps helpful during cellular penetration.

The use of ruthenium and rhodium could be interesting as a potentially less toxic alternative to platinum [47, 48]. The results reported herein indicate that organometallic compounds showed potent antibacterial activity against a representative group of bacteria. This may support acceptance for organometallics in pharmaceutical industries and further research in this area and their biological targets. Therefore, the activity of these compounds offers opportunities in the superbug age.

Acknowledgements

Authors are grateful to acknowledge Head, Department of Chemistry, Govt. Science College, Jabalpur for providing laboratory facilities. Thanks are also due to SAIF, CDRI, Lucknow and SAIF, Pondicherry University, Pondicherry for recording spectra and elemental data. RM is thankful to Dr J.J. Ahire, Postdoc Fellow, University of Stellenbosch, South Africa, for his kind help in statistical analysis.

References

[1] G. Gasser, I. Ott, N.M. Metzler-Nolte. *J. Med. Chem.*, **54**, 3 (2011).
[2] P.J. Dyson, G. Sava. *Dalton Trans.*, 1929 (2006).
[3] T. Gianferrara, I. Bratsos, E. Alessio. *Dalton Trans.*, 7588 (2009).
[4] G. Jaouen. *Bioorganometallics: Biomolecules Labeling, Medicine*, Wiley-VCH, Weinheim (2006).
[5] T. Kawamoto. *Inorg. Chim. Acta*, **300–302**, 512 (2000).
[6] P. Ghosh, A. Pramanik, N. Bag, G.K. Lahiri, A. Chakravorty. *J. Organomet. Chem.*, **454**, 237 (1993).
[7] P.K. Gogoi, G. Borah, N. Bharali, D. Saikai. *Ind. J. Chem.*, **46A**, 1113 (2007).
[8] N. Sathya, A. Manimaran, G. Raja, P. Muthusamy, K. Deivasigamani, C. Jayabalakrishnan. *Transition Met. Chem.*, **34**, 7 (2009).
[9] T.H. Lowry, K.S. Richardson. *Mechanism and Theory in Organic Chemistry*, 166, Harper & Row, New York (1976).
[10] R.G. Pearson. *J. Am. Chem. Soc.*, **85**, 3533 (1963).
[11] R.G. Pearson, J. Songstad. *J. Am. Chem. Soc.*, **89**, 1827 (1967).
[12] M.I. Bruce, M.Z. Iqbal, F.G.A. Stone. *J. Organomet. Chem.*, **31**, 275 (1971).
[13] A.J. Klaus, P. Rys. *Helv. Chim. Acta*, **64**, 1452 (1981).
[14] K. Gehrig, M. Hugentobler, A.J. Klaus, P. Rys. *Inorg. Chem.*, **21**, 2493 (1982).
[15] G.K. Lahiri, S. Bhattacharya, B.K. Ghosh, A. Chakravorty. *Inorg. Chem.*, **26**, 4324 (1987).
[16] J. Chakravarty, S. Bhattacharya. *Polyhedron*, **15**, 257 (1996).
[17] N.C. Pramanik, S. Bhattacharya. *Polyhedron*, **16**, 1755 (1997).
[18] P. Paul, S. Bhattacharya. *J. Chem. Sci.*, **124**, 1165 (2012).
[19] J.A. Osborn, J.F. Jardine, J.F. Young, G. Wilkinson. *Inorg. Synth.*, **10**, 67 (1967).
[20] J. Chatt, G. Leigh, D.M.P. Mingos, R.J. Paske. *J. Chem. Soc. (A)*, 2636 (1968).
[21] R. Mehrotra, S.N. Shukla, P. Gaur. *J. Coord. Chem.*, **65**, 176 (2012).
[22] W.J. Geary. *Coord. Chem. Rev.*, **7**, 81 (1971).
[23] R. Ramesh, S. Maheswaran. *J. Inorg. Biochem.*, **96**, 457 (2003).

[24] K.D. Keerthi, B.K. Santra, G.K. Lahiri. *Polyhedron*, **17**, 1387 (1998).
[25] R. Mehrotra, S.N. Shukla, P. Gaur, A. Dubey. *Eur. J. Med. Chem.*, **50**, 149 (2012).
[26] S.N. Shukla, P. Gaur, R. Mehrotra, M. Prasad, H. Kaur, M. Prasad, R.S. Srivastava. *J. Coord. Chem.*, **62**, 2556 (2009).
[27] R.M. Silverstein, G.C. Bassler, T.C. Morrill. *Spectrometric Identification of Organic Compounds*, 104, Wiley, New York (1991).
[28] S. Dutta, S.M. Peng, S. Bhattacharya. *Dalton Trans.*, 4623 (2000).
[29] A. Das, F. Basuli, S.M. Peng, S. Bhattacharya. *Polyhedron*, **18**, 2729 (1999).
[30] B.R. James, R.H. Morris. *Can. J. Chem.*, **58**, 399 (1980).
[31] T. Bora, M.M. Singh. *Transition Met. Chem.*, **3**, 27 (1978).
[32] A.B.P. Lever. *Inorganic Electronic Spectroscopy*, 2nd Edn, Elsevier, Amsterdam (1984).
[33] S.N. Shukla, P. Gaur, A. Dubey, S. Mathews, R. Mehrotra. *J. Coord. Chem.*, **65**, 602 (2012).
[34] V.K. Sharma, A. Srivastava, S. Srivastava. *J. Serb. Chem. Soc.*, **71**, 917 (2006).
[35] A.C. Chen, L. Ren, A. Decken, C.M. Crudden. *Organometallics*, **19**, 3459 (2000).
[36] S.N. Shukla, P. Gaur, H. Kaur, M. Prasad, R. Mehrotra, R.S. Srivastava. *J. Coord. Chem.*, **61**, 441 (2008).
[37] A. Rattan. In *Antimicrobials in Laboratory Medicine*, Vol. 85, B.I. Churchill Livingstone, New Delhi (2000).
[38] N. Raman, J.D. Raja. *Ind. J. Chem.*, **46A**, 1611 (2007).
[39] R. Mehrotra, S.N. Shukla, P. Gaur. *Med. Chem. Res.*, **21**, 4455 (2012).
[40] S.N. Shukla, P. Gaur, N. Rai, R. Mehrotra. *J. Chin. Chem. Soc.*, **61**, 594 (2014).
[41] C.P. Tan, J. Liu, L.M. Chen, S. Shi, L.N. Ji. *J. Inorg. Biochem.*, **102**, 1644 (2008).
[42] R. Mehrotra, S.N. Shukla, P. Gaur. J. Serb. *Chem. Soc.* (in press), doi: 10.2298/JSC140704086M.
[43] M. Frezza, Q.P. Dou, Y. Xiao, H. Samouei, M. Rashidi, F. Samari, B. Hemmateenejad. *J. Med. Chem.*, **54**, 6166 (2011).
[44] C.P. Bagowski, Y. You, H. Scheffler, D.H. Vlecken, D.J. Schmitz, I. Ott. *Dalton Trans.*, 10799 (2009).
[45] T. Giraldi, G. Sava, G. Bertoli, G. Mestroni, G. Zassinovich. *Cancer Res.*, **37**, 2662 (1977).
[46] A. Ciric, R. Jelic, L. Joksovic, M.J. Stankov, P. Djurdjevic. *Can. J. Anal. Sci. Spectrosc.*, **52**, 343 (2007).
[47] B.M. Zeglis, V.C. Pierre, J.K. Barton. *Chem. Commun.*, 4565 (2007).
[48] C.S. Allardyce, P.J. Dyson. *Plat. Met. Rev.*, **45**, 62 (2001).